Baseline Assessment of Circulating MicroRNAs Near Diagnosis of Type 1 Diabetes Predicts Future Stimulated Insulin Secretion

Isaac Snowhite,[1] Ricardo Pastori,[1,2] Jay Sosenko,[2] Shari Messinger Cayetano,[3] and Alberto Pugliese[1,2,4]

Diabetes 2021;70:638–651 | https://doi.org/10.2337/db20-0817

Type 1 diabetes is an autoimmune disease resulting in severely impaired insulin secretion. We investigated whether circulating microRNAs (miRNAs) are associated with residual insulin secretion at diagnosis and predict the severity of its future decline. We studied 53 newly diagnosed subjects enrolled in placebo groups of TrialNet clinical trials. We measured serum levels of 2,083 miRNAs, using RNA sequencing technology, in fasting samples from the baseline visit (<100 days from diagnosis), during which residual insulin secretion was measured with a mixed meal tolerance test (MMTT). Area under the curve (AUC) C-peptide and peak C-peptide were stratified by quartiles of expression of 31 miRNAs. After adjustment for baseline C-peptide, age, BMI, and sex, baseline levels of miR-3187-3p, miR-4302, and the miRNA combination of miR-3187-3p/miR-103a-3p predicted differences in MMTT C-peptide AUC/peak levels at the 12-month visit; the combination miR-3187-3p/miR-4723-5p predicted proportions of subjects above/below the 200 pmol/L clinical trial eligibility threshold at the 12-month visit. Thus, miRNA assessment at baseline identifies associations with C-peptide and stratifies subjects for future severity of C-peptide loss after 1 year. We suggest that miRNAs may be useful in predicting future C-peptide decline for improved subject stratification in clinical trials.

Type 1 diabetes is a chronic autoimmune disease leading to progressive (yet heterogeneous) loss and dysfunction of pancreatic β-cells (1). The TrialNet organization has completed clinical trials in participants with newly diagnosed type 1 diabetes (<100 days) and stimulated peak C-peptide >200 pmol/L. A 2-year follow-up of 191 participants in placebo groups demonstrated greater C-peptide loss during the 1st year postdiagnosis (2), yet 88% and 66% had stimulated peak C-peptide ≥200 pmol/L 1 year and 2 years after diagnosis, respectively. Several agents preserve insulin secretion in individuals with newly diagnosed type 1 diabetes, in some cases for up to 2–7 years after treatment (3). Novel biomarkers to stratify trial participants at baseline and predict decline of their insulin secretion would afford gains in trial design and efficiency, facilitating the identification of effective therapies.

MicroRNAs (miRNAs) are small, noncoding RNAs that regulate gene expression (4) and are emerging as disease biomarkers. Circulating miRNAs are stable and measurable in serum and plasma with similar results (5). Twenty-nine circulating miRNAs were associated with type 1 diabetes by two to eight studies (6–24) (Supplementary Table 1), suggesting reproducible associations despite heterogeneity in study design, cohorts, assays, and analysis methods. Cellular miRNAs were also linked to both human and experimental diabetes (23,25–30).

An outstanding question is whether circulating miRNAs predict C-peptide decline after diagnosis. Samandari et al. (12) assessed plasma levels using Exiqon RT-PCR assays for 179 miRNAs and found that 3-month visit plasma levels of several miRNAs (miR-24-3p, miR-146a-5p, miR-194-5p, miR-197-3p, miR-301a-3p, and miR-375) correlated with residual β-cell function at the 6- and 12-month visits; miR-197-3p levels at the 3-month visit predicted β-cell function

[1]Diabetes Research Institute, Leonard M. Miller School of Medicine, University of Miami, Miami, FL
[2]Division of Endocrinology and Metabolism, Department of Medicine, Leonard M. Miller School of Medicine, University of Miami, Miami, FL
[3]Department of Public Health Sciences, Leonard M. Miller School of Medicine, University of Miami, Miami, FL
[4]Department of Microbiology and Immunology, Leonard M. Miller School of Medicine, University of Miami, Miami, FL

Corresponding author: Alberto Pugliese, apuglies@med.miami.edu

Received 7 August 2020 and accepted 24 November 2020

This article contains supplementary material online at https://doi.org/10.2337/figshare.13281188.

12 months after diagnosis. Garavelli et al. (24) reported that miR-23a-3p, miR-23b-3p, miR-24-3p, miR-27a-3p, and miR-27b-3p predicted fasting C-peptide loss of <10% or >90% 12 months after diagnosis. In other studies, Let-7g was associated with C-peptide levels during the 1st year postdiagnosis (19), levels of the β-cell–enriched miR-204 correlated with C-peptide area under the curve (AUC) at diagnosis (31), and levels of miR-142-5p, miR-29c-3p, and miR-320 differed in children with recent-onset type 1 diabetes according to residual fasting C-peptide (23).

We assessed levels of 2,083 miRNAs in baseline serum samples from 53 participants with newly diagnosed type 1 diabetes randomized to placebo groups in TrialNet clinical trials. We report miRNA associations with stimulated C-peptide, which are maintained at the 12-month visit and stratify participants for future severity of C-peptide loss.

RESEARCH DESIGN AND METHODS

Subjects

We examined baseline serum samples from 53 individuals with newly diagnosed type 1 diabetes who were enrolled in TrialNet clinical trial placebo groups <100 days from diagnosis and with stimulated peak C-peptide >200 pmol/L. Table 1 shows their baseline characteristics. Subjects were included in this study on the basis of availability of a fasting serum sample that could be used for miRNA assessment obtained on the day of the baseline mixed meal tolerance test (MMTT). Supplementary Fig. 1 illustrates C-peptide AUC and peak levels during the 2-h MMTTs performed at the baseline, 6-month, and 12-month visits (2). The baseline MMTT was performed within an average ± SD of 1.9 ± 0.1 months from diagnosis, or 58 days.

MMTT

The MMTT was described previously (32). Serum C-peptide levels were measured using a TOSOH AIA-900 Automated Immunoassay Analyzer. The trapezoidal rule was used to calculate the C-peptide AUC in nmol/L; peak levels are reported in pmol/L (2).

miRNA Assay

We tested 15-μL serum aliquots. Samples were collected and processed according to TrialNet protocols (Supplementary Material). miRNAs were assayed using the HTG EdgeSeq miRNA Whole Transcriptome Assay (HTG Molecular Diagnostics) (33), which combines a quantitative nuclease protection assay with next-generation sequencing. It does not require miRNA isolation, reverse transcription, adenylation, or ligation, which could introduce bias. The assay has a broad dynamic range with high reproducibility, sensitivity, and specificity (33). Testing of blind replicate samples from four individuals with type 1 diabetes provided by the JDRF Biomarker Working Group Core for Assay Validation confirmed excellent reproducibility (r = 0.94–0.96; coefficient of variation 1.06%). Undiluted RNA is bound to corresponding target-specific nuclease protection probes after treatment with lysis buffer. The probe set contains complementary sequences for 2,083 specific miRNAs or ~78% of the published mature transcripts in miRBase V22 (34). Probes hybridized to cognate miRNAs are protected from S1 nuclease digestion, amplified with the addition of barcodes, and sequenced. After amplification, the library was quantified according to the HTG EdgeSeq KAPA library quantification protocol for Illumina sequencing.

Sample Processing and Batch Control

Processing controls include four negative and one positive control and a human brain RNA standard. All samples were run as singletons, except the standard was run in triplicate. Samples were randomized before placement to reduce interplate and intraplate biases, which were assessed using both Pearson and Spearman correlation coefficients.

Postsequencing Quality Control

Each well in HTG EdgeSeq assays included four negative control probes and one positive control probe with unique sequences. All samples and controls were quantified in triplicate with the inclusion of no template control reactions during the quantitative PCR process. A PhiX control adaptor-ligated library was spiked into the pooled library to confirm labeling efficiency, and each well was spiked with four unique plant sequences that were digested by the S1 nuclease during the protection assay.

miRNA Data Management and Analysis

The output was a read count, as in small RNA sequencing (RNA-seq), but unlike small RNA-seq, the read count reflects the quantity of probes bound by miRNAs and protected from digestion. The HTG EdgeSeq Parser aligned the FASTQ files to the probe list to collate the data. Data tables included raw, quality control raw, $\log_2$ counts per million (CPM), and median normalized.

CPM Standardization and Normalization

CPM standardization was used for evaluation between samples, replicate comparisons, batch effects, and quality control metrics. The $\log_2$ transformation was used for standardizing, or scaling, gene-level data within a sample. CPM standardization allows the evaluation of probe-level expression as a proportion of total counts on a sample level and between samples, as described in the limma package (35,36). Intersample normalization was achieved by scaling raw read counts in each lane by a single lane-specific factor reflecting its library size (37). Gene counts were divided by the median of mapped reads (or library size) associated with their lane and multiplied by the median total count across all samples. Normalization was performed using the DESeq2 package from Bioconductor and the R statistical program (https://www.r-project.org).

Statistical Analysis

We investigated whether C-peptide levels (fasting, AUC, and peak) were associated with miRNA levels at the baseline MMTT. We next examined whether baseline associations were maintained at the 12-month MMTT.

Table 1—Baseline characteristics of 53 subjects with new-onset type 1 diabetes

	Value
Subjects, *N*	53
Male/female sex, *n*	34/19
TrialNet trials, *N* (males/females)	
TN02 MMF/DZB	16 (11/5)
TN08 GAD	19 (12/7)
TN09 CTLA-4Ig	8 (6/2)
TN14 Anti-IL-1β	10 (5/5)
Age of diagnosis (years)	16.8 ± 10.0
Type 1 diabetes duration at MMTT (months)	1.9 ± 0.1
BMI (kg/m^2)	20.8 ± 4.2
HbA_{1c}	
mmol/mol	60 ± 26
%	7.6 ± 1.7
2-h MMTT	
Fasting C-peptide (pmol/L)	364.1 ± 216.3
AUC C-peptide (nmol/L)	82.2 ± 35.3
Peak C-peptide (pmol/L)	886.2 ± 385.1
Fasting glucose (mmol/L)	112.8 ± 29.6
Peak glucose (mmol/L)	2.7 ± 1.2

Data are mean ± SD unless otherwise indicated. Essential baseline characteristics of the study cohort and baseline MMTT C-peptide outcomes are shown.

Baseline Analysis

We estimated associations between baseline MMTT outcomes (fasting C-peptide, AUC, and peak levels) and miRNA levels. For each miRNA, we fit a linear model to MMTT outcomes, including a nominal indicator of quartile of expression, with adjustments for age, BMI, and sex. Global *F* tests of significance determined a list of miRNAs where variability in baseline MMTT outcome was significantly explained by miRNA quartile. Bootstrapped resampling with 1,000 replications provided correction for multiple comparisons and estimated comparisons among quartiles for differences in MMTT outcomes. For those miRNAs having significant bootstrapped associations between expression quartiles and MMTT outcomes, we evaluated specific comparisons between quartiles for significant differences in MMTT outcomes.

Longitudinal Analysis

Those miRNAs with baseline associations with MMTT outcomes were investigated to evaluate maintained associations with 12-month C-peptide AUC and peak. This was accomplished by fitting a linear model to each MMTT, considering quartile of miRNA expression with identified association with baseline MMTT, and adjusting for corresponding baseline C-peptide, age at draw, sex, and BMI. Results illustrating evidence of longitudinal associations with specific miRNAs were then considered in stepwise regression to identify those miRNAs that, in combination, had significant association and best predicted 12-month MMTT after adjustment for baseline C-peptide AUC, age, sex, and BMI.

Receiver Operating Characteristic Curves

Receiver operating characteristic (ROC) curves were constructed from predicted values from logistic regression models fit to binary outcome defined by percentage decline from baseline (<25% vs. >25%). These models were fit with/without miRNA information in addition to baseline C-peptide AUC and were adjusted for BMI and sex. ROC curves were compared to determine whether miRNAs improved prediction of C-peptide decline above the baseline C-peptide AUC using the DeLong test for correlated ROC curves (38).

Longitudinal Assessment of MMTT C-Peptide/Glucose Response Curves After Stratification for Baseline miRNA Levels

We plotted glucose against C-peptide values (30–120 min) from baseline, 6-month, and 12-month MMTTs for the two groups of subjects defined by baseline miRNA levels. Changes/differences in the curves' position (shifts to the left, lower C-peptide; upward, higher glucose), directionality, and shape (a narrower horizontal spread and upward straightening of the curve or a monotonic shape) illustrate progressive worsening over time and differences between miRNA-stratified groups. We used the *t* test to assess statistical significance in comparisons of baseline mean AUC C-peptide/AUC glucose ratios of the two miRNA expression groups (curves) with 6- and 12-month ratios and in comparisons of miRNA-stratified groups (curves) within each MMTT.

Other Analyses

For statistical comparisons involving binary outcomes, groups were compared using the two-tailed Fisher exact test.

Bioinformatic Prediction of Putative Gene Targets and Pathways

We interrogated the reference Kyoto Encyclopedia of Genes and Genomes database (https://www.genome.jp/kegg) and used miRWalk 2.0 (39) (http://zmf.umm.uni-heidelberg.de/apps/zmf/mirwalk2) to identify gene pathways predicted to be targeted by miRNAs of interest (accessed April–May 2020). miRWalk 2.0 hosts predicted and experimentally validated miRNA-target interaction pairs, documents miRNA-binding sites within the complete sequence of a gene, and combines this information with a comparison of binding sites resulting from use of miRanda-rel2010, TargetScan 6.2, miRWalk 2.0, and RNA22 v2. Statistical significance of these predictions is reported after the Benjamini-Hochberg correction for multiple comparisons.

Data and Resource Availability

The data sets generated and/or analyzed during the current study were deposited in the Gene Expression Omnibus repository (https://www.ncbi.nlm.nih.gov/geo/query/acc.cgi?acc=GSE157177). No applicable resources were generated or analyzed during the current study.

RESULTS

Detection of miRNAs

The EdgeSeq assays collectively detected all 2,083 miRNAs. Detection rates were >95% for all but four miRNAs

Table 2—miRNAs associated with baseline MMTT AUC and/or peak C-peptide

miRNA	Quartile comparison	C-peptide AUC estimated difference (nmol/L)	*P* value	C-peptide peak estimated difference (pmol/L)	*P* value
Associated with AUC and peak C-peptide					
miR-3187-3p	Q2–4 vs. Q1	42.30	0.0018	442	0.0070
miR-4302	Q2–4 vs. Q1	35.19	0.0218	344	0.0065
miR-8079	Q2–4 vs. Q1	34.46	0.0156	387	0.0258
miR-197-3p	Q1 vs. Q2–4	33.58	0.0150	351	0.0086
miR-193b-5p	Q2–4 vs. Q1	32.58	0.0272	366	0.0178
miR-4669	Q2–4 vs. Q1	31.75	0.0279	351	0.0419
miR-494-5p	Q1–3 vs. Q4	31.72	0.0233	325	0.0377
miR-103a-3p	Q1 vs. Q2–4	31.44	0.0231	332	0.0560
miR-4304	Q1–3 vs. Q4	29.83	0.0257	324	0.0360
miR-4701-3p	Q1–3 vs. Q4	29.75	0.0269	272	0.0501
miR-98–3p	Q2–4 vs Q1	29.23	0.0387	337	0.0480
miR-99a-5p	Q4 vs. Q1–3	28.42	0.0367	312	0.0492
miR-3678-3p	Q1–3 vs. Q4	27.77	0.0292	290	0.0487
miR-5682	Q1–3 vs. Q4	26.91	0.0436	288	0.0343
miR-7154-3p	Q1–3 vs. Q4	26.55	0.0457	294	0.0194
miR-3191-3p	Q1–3 vs. Q4	26.14	0.0455	276	0.0106
Associated with C-peptide AUC					
miR-8058	Q2–4 vs. Q1	32.30	0.0216	—	NS
miR-2355-3p	Q1–3 vs. Q4	32.13	0.0162	—	NS
miR-934	Q2–4 vs. Q1	28.77	0.0443	—	NS
miR-6748-3p	Q1 vs. Q2–4	28.71	0.0275	—	NS
miR-6073	Q1–3 vs. Q4	28.33	0.0416	—	NS
miR-342-3p	Q4 vs. Q1–3	26.96	0.0572	—	NS
miR-622	Q2–4 vs. Q1	26.92	0.0369	—	NS
miR-215-5p	Q2–4 vs. Q1	26.89	0.0563	—	NS
miR-568	Q1–3 vs. Q4	25.92	0.0456	—	NS
Associated with peak C-peptide					
miR-1208	Q2–4 vs. Q1	—	NS	361	0.0406
miR-1292-5p	Q2–4 vs. Q1	—	NS	311	0.0326
miR-589-5p	Q1–3 vs. Q4	—	NS	297	0.0159
miR-4723-5p	Q2–4 vs. Q1	—	NS	283	0.0260
miR-127-3p	Q1 vs. Q2–4	—	NS	282	0.0321
miR-6506-5p	Q1–3 vs. Q4	—	NS	281	0.0559

Reported are estimated differences in C-peptide levels between subject groups defined by quartiles of miRNA expression. Estimated differences and *P* values are corrected for multiple comparisons by bootstrapping analysis. The estimated differences are those between the quartile comparisons; the quartiles on the left side of the comparison are those associated with higher C-peptide AUC or peak levels. Either the highest or the lowest quartile of miRNA expression was associated with higher or lower C-peptide levels compared with the remaining quartiles, which did not differ among themselves. C-peptide AUC and peak levels showed associations with 16 miRNAs, and miRNAs are ranked by the estimated difference in C-peptide AUC; 9 miRNAs were associated with AUC and 6 miRNAs with peak C-peptide, and miRNAs are ranked by estimated difference in AUC or peak.

(miR-128-2-5p 2%, miR-1282 27%, miR-4525 6%, miR-6752-3p 38%). The average ± SD detection rate was 2,077 ± 12 miRNAs, which accounts for 99.7 ± 0.5% of the panel. The mean normalized $\log_2$ CPM values were 7.92 ± 0.33 (range 0.5–22.4) for all miRNAs. We observed very robust raw counts (mean 3.2 ± 1.05, range 1.4–7.7 million reads) in 15 μL of serum.

Baseline Associations

We estimated associations of baseline MMTT outcomes (fasting C-peptide, AUC, and peak levels) with miRNA expression quartiles. Bootstrapped resampling with 1,000 replications provided adjusted *P* values for associated miRNAs to correct for multiple comparisons and estimated comparisons among quartiles for differences in MMTT outcomes. Among statistically significant associations of C-peptide with mRNAs after bootstrapping, lowest or highest quartiles versus the other three quartiles were generally best at discriminating C-peptide differences. Table 2 lists miRNAs and quartile comparisons that identified significant differences in baseline C-peptide AUC and/or peak. Differences in C-peptide AUC or peak were identified by 25 and 22 miRNAs, respectively, among which 16 miRNAs had associations with both outcomes, which are naturally correlated. There were nine and six miRNAs associated with either C-peptide AUC or peak levels. There were no significant miRNA associations with fasting C-peptide. miRNA expression quartiles identified baseline C-peptide AUC differences ranging from 25.92 to 42.3 nmol/L and peak C-peptide differences ranging from 276 to 442 pmol/L after bootstrapping. The miRNA that identified the largest C-peptide AUC and peak

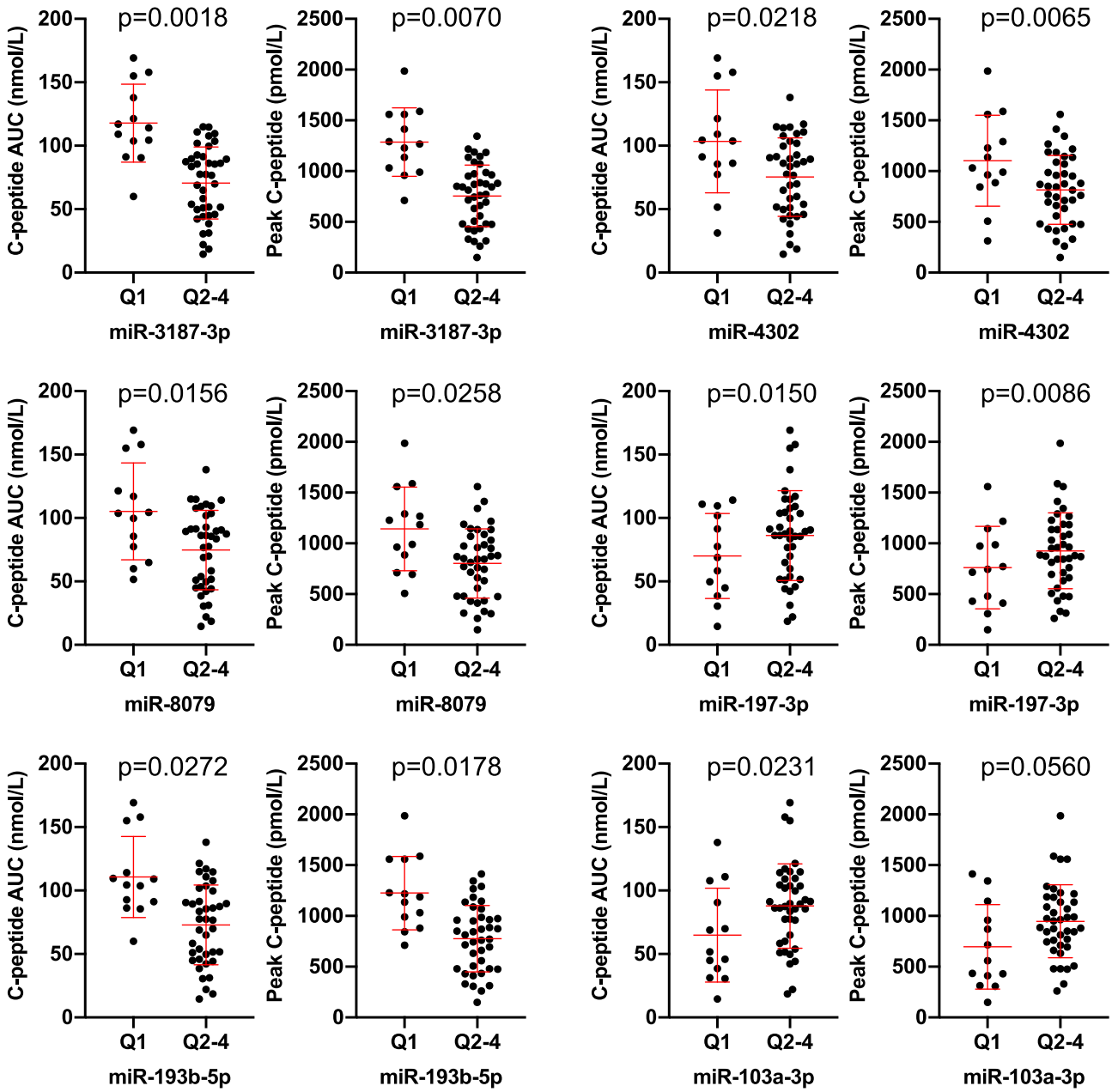

Figure 1—Baseline miRNA quartile-level association with baseline C-peptide AUC and peak levels. Illustrated are individual C-peptide AUC and peak levels according to miRNA expression quartiles. Data are mean ± SD and shown for six representative miRNAs. Differences between groups and *P* values after bootstrapping are reported from Table 2. Q, quartile.

differences was miR-3187-3p (42.3 nmol/L and 442 pmol/L, respectively); the previously reported miR-197-3p (6) identified C-peptide AUC and peak differences of 33.58 nmol/L and 351 pmol/L, respectively. All values are reported in Table 2. Figure 1 shows C-peptide AUC and peak levels according to miRNA expression quartiles for six representative miRNAs. Supplementary Table 5 reports total raw counts, raw CPM, and normalized CPM ($\log_2$) for the 31 miRNAs associated with C-peptide.

Longitudinal Associations

We investigated whether baseline miRNAs predicted C-peptide at the 12-month MMTT. Specifically, we examined whether any miRNA associated with baseline C-peptide AUC and/or peak (Table 2) remained associated and predicted C-peptide AUC and/or peak at the 12-month MMTT after adjusting for baseline C-peptide, age, sex, and BMI. Two miRNAs remained associated with both C-peptide AUC (miR-3187-3p $P = 0.037$, miR-4302 $P = 0.047$) and peak (miR-3187-3p $P = 0.038$, miR-4302 $P = 0.039$) at the 12-month MMTT (Table 3). Baseline expression quartiles of miR-3187-3p and miR-4302 defined groups of participants with a mean difference in the 12-month C-peptide AUC of 22.49 and 21.05 nmol/L, respectively; mean differences for 12-month peak C-peptide were 236 and 229 pmol/L, respectively. miR-1292-5p was associated with peak

Table 3—miRNAs assessed at baseline with association with C-peptide AUC and/or peak at the 12-month MMTT

miRNA	Quartile comparison	C-peptide AUC estimated difference (nmol/L)	*P* value	C-peptide peak estimated difference (pmol/L)	*P* value
miR-3187-3p	Q2–4 vs. Q1	22.49	0.0371	236	0.0383
miR-4302	Q2–4 vs. Q1	21.05	0.0479	229	0.0391
miR-1292-5p	Q2–4 vs. Q1	—	—	212	0.0496

Reported are estimated differences in the 12-month MMTT C-peptide levels between subject groups defined by baseline quartiles of miRNA expression. The estimated differences are those between the quartile comparisons, as described in the legend of Table 2.

C-peptide only (mean difference 212 pmol/L). Figure 2 illustrates longitudinal associations and C-peptide decline for representative miRNAs miR-3187-3p and miR-4302 (which stratified subjects with significantly different 12-month C-peptide AUC and peak) and miR-103a-3p and miR-197-3p (which stratified subjects only at baseline).

Stepwise Regression Modeling to Identify Combinations of Predictive miRNAs

miRNAs associated with baseline C-peptide AUC were evaluated in a stepwise regression to identify miRNA combinations with improved prediction of 12-month C-peptide AUC after adjustment for baseline C-peptide AUC, age, sex, and BMI. Twelve of 25 miRNAs with baseline associations were included in the model. The combination of miR-3187-3p and miR-103a-3p discriminated C-peptide AUC (Fig. 3*A*) and peak levels (Fig. 3*B*) at 12 months. Stratification according to baseline miRNA expression quartiles for this combination demonstrated differences in the baseline to 12-month AUC and peak C-peptide levels of 37.95 nmol/L ($P = 0.001$) and 39 pmol/L ($P = 0.001$) between groups (Supplementary Table 2). Eleven subjects with low expression (first quartile) of miR-3187-3p combined with high expression (second–fourth quartile) of miR-103a-3p had higher 12-month C-peptide AUC compared with the other 42 subjects. This combination was superior to miR-3187-3p alone because two more subjects were stratified to the lower C-peptide group. The miR-3187-3p/miR-4302 combination identified differences in AUC C-peptide decline of 44.86 nmol/L ($P = 0.001$) (Fig. 3*C* and Supplementary Table 2) and assigned two additional individuals to the lower C-peptide group than miR-3187-3p alone.

We also investigated whether any single miRNA or combination could stratify subjects at the 12-month visit by peak C-peptide levels above/below the clinical trial eligibility threshold. No individual miRNA from Table 2 was predictive. However, the combination of miR-3187-3p and miR-4723-5p predicted that 94% (17 of 18) of the participants with baseline expression levels in the lower quartile for both miRNAs would have a peak C-peptide level >200 pmol/L at the 12-month visit compared with 64% (22 of 34) of those with miRNA expression levels in the second to fourth quartiles ($P = 0.021$ by two-tailed Fisher exact test, relative risk 1.4 [95% CI 1.086–1.993], sensitivity 0.4359 [95% CI 0.2930–0.5902], specificity 0.9231 [95% CI 0.6669–0.9961]).

We examined whether miRNAs improved prediction of C-peptide decline compared with baseline C-peptide AUC. The ROC curve in Fig. 3*D* illustrates an improved ability to separate between groups with decline greater/lower than 25% when the miR-3187-3p/miR-103a-3p combination is considered in the model; ROC AUCs with/without miRNAs were 0.82 and 0.70, respectively ($P = 0.04$).

Longitudinal Assessment of MMTT C-Peptide/Glucose Response Curves After Stratification for Baseline miRNA Levels

C-peptide/glucose response curves for baseline, 6-month, and 12-month MMTTs stratified subjects into two groups (curves) by their baseline levels of associated miRNAs (Fig. 4). Curves evolved at 6 months and 12 months, demonstrating progressive worsening of insulin secretion (shift to the left) and higher glucose levels (shift upward), with greater separation of the curves for the miRNA combinations. Overall, subject stratification by baseline miRNA expression quartiles demonstrated differences in disease severity at diagnosis that persisted during further progression and involved both C-peptide and glucose responses.

Longitudinally, we compared baseline mean AUC C-peptide/AUC glucose ratios of the two miRNA expression groups (curves) with the ratios of the corresponding curves at later time points; for example, the ratio from the first quartile curve at baseline was compared with the ratio of the first quartile curve at 6 months, and the same comparison was made between 6 and 12 months. These were all significantly different from one another, demonstrating worsening in both groups (range $P < 0.0001$–0.02 by two-tailed paired *t* test) (Supplementary Table 3). However, 6- and 12-month curves of miR-3187-3p/miR-4302 were statistically different from each other for subjects in combination group 0 but not for those in combination group 1, suggesting that the latter did not experience significant worsening in this time interval. Cross-sectionally, we compared AUC C-peptide/AUC glucose ratios of the two groups (curves) in each panel; these were significantly different at all time points for all miRNAs or combinations analyzed (range $P < 0.0001$–0.0397 by two-tailed unpaired *t* test) (Supplementary Table 4); the

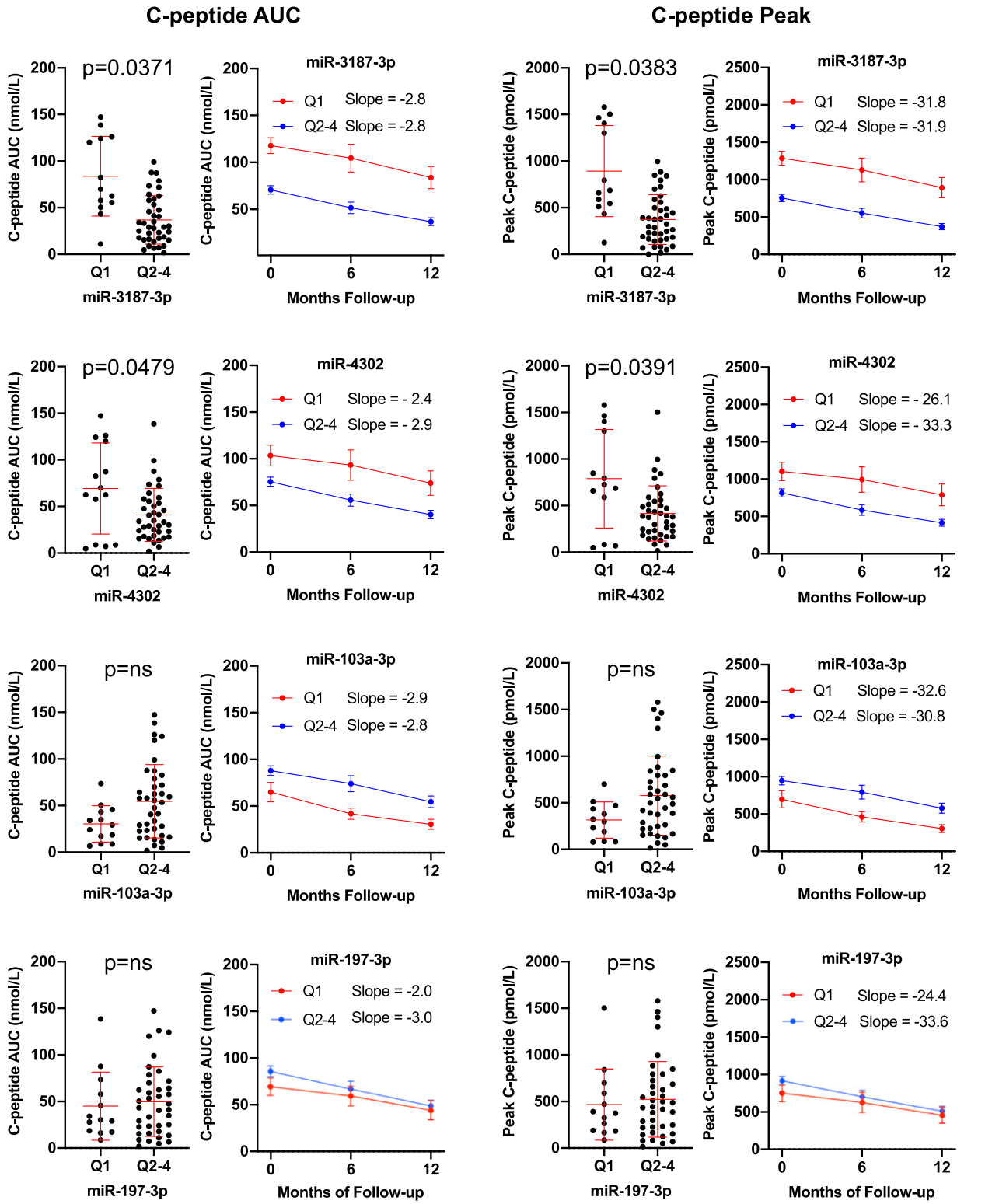

Figure 2—Baseline miRNA levels association with 12-month C-peptide AUC and peak levels. The dot plots illustrate C-peptide AUC and peak levels at the 12-month visit for participants stratified by baseline miRNA expression quartiles. Their C-peptide AUC and peak values are shown from baseline to the 12-month visit, and slope values are reported. Data are mean ± SD and shown for four representative miRNAs. The baseline associations of miR-3187-3p and miR-4302 with C-peptide values remained significant at the 12-month visit for which differences between groups and *P* values are reported from Table 3. The baseline levels of miR-103a-3p and miR-197-3p were not associated with statistically significant C-peptide differences at the 12-month visit. Q, quartile.

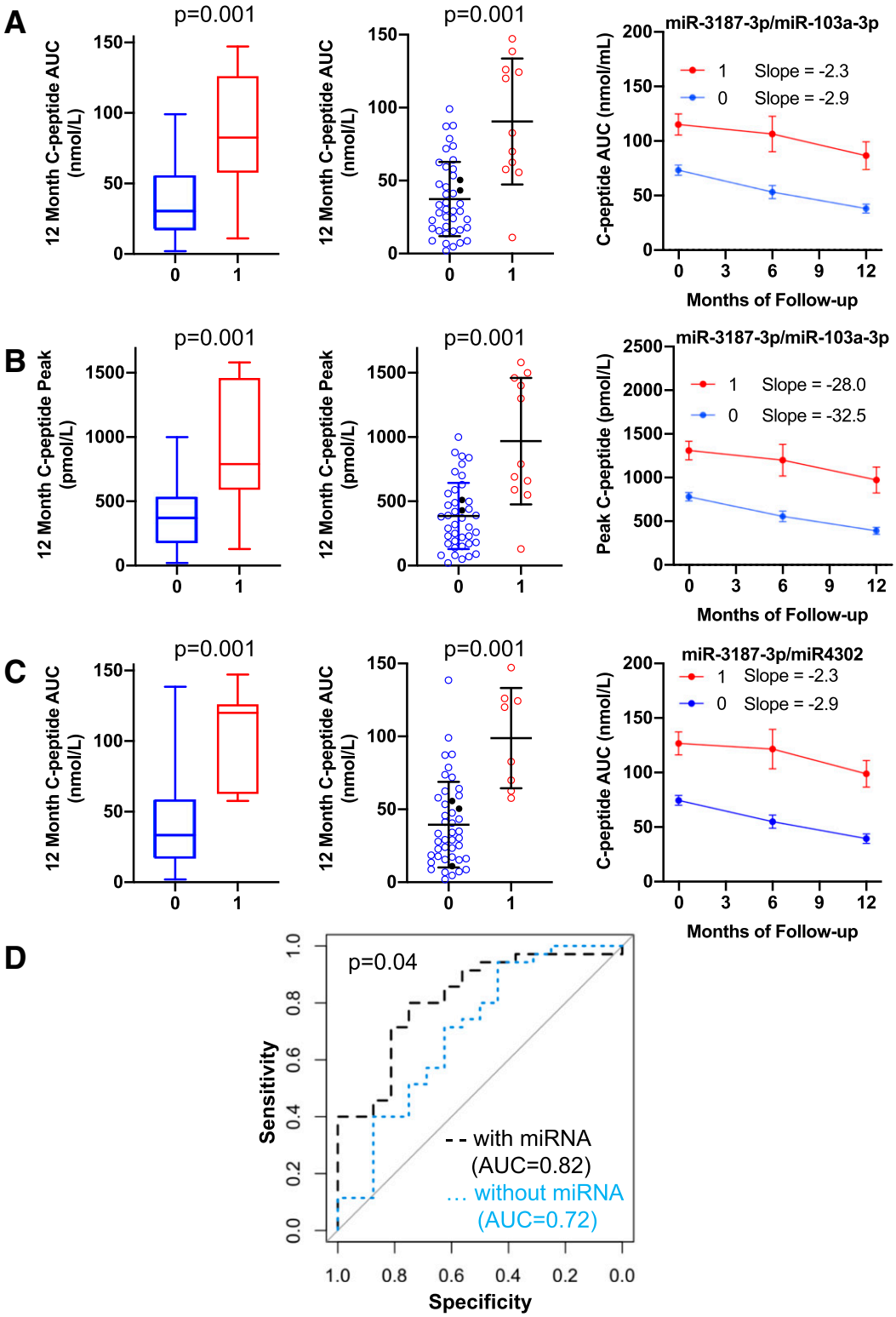

Figure 3—Combined baseline levels of selected miRNAs predict C-peptide at the 12-month visit. *A–C*: The 12-month AUC (*A* and *C*) and peak C-peptide (*B*) in subject groups defined by baseline combined levels of miR-3187-3p and miR-103a-3p (*A* and *B*) or miR-3187-3p and miR-4302 (*C*). The box and whiskers show median, first and fourth quartiles, and maximum/minimum values. The dot plots show individual values, means, and SDs. Black circles in the dot plots mark subjects with lower C-peptide outcome uniquely identified by the miRNA combinations. By multivariable analysis, the miR-3187-3p/miR-103a-3p combination identified differences between groups in AUC and peak C-peptide decline from baseline to 12 months of 37.95 nmol/L ($P = 0.001$) and 39 pmol/L ($P = 0.001$), respectively. Likewise, the miR-3187-3p/miR-4302 combination identified differences between groups in AUC C-peptide decline of 44.86 nmol/L ($P = 0.001$). In *A* and *B*, combination 0 = quartile 1 (Q1) miR-103a-3p + Q2–4 miR-3187-3p, and combination 1 = Q2–4 miR-103a-3p + Q1 miR-3187-3p; in *C*, combination 0 = Q2–4 miR-3187-3p + Q2–4 miR-4302, and combination 1 = Q1 miR-3187-3p + Q1 miR-4302. Results of these analyses

only exception was the miR-103a-3p 12-month curves ($P = 0.05$). The findings suggest significant differences in disease progression identified by stratification in groups defined by baseline miRNA levels.

Bioinformatic Prediction of Target Gene Pathways

We used miRWalk 2.0 (39) to examine whether any of the 31 miRNAs associated with C-peptide AUC and/or peak at baseline are predicted to modulate gene pathways relevant to type 1 diabetes. Results are reported in Table 4 where we list four major gene pathways relevant to type 1 diabetes and/or type 2 diabetes, specifically the insulin signaling, SNARE interactions in vesicular transport, type 2 diabetes, and the T-cell receptor (TCR) signaling pathways. Nineteen miRNAs were predicted to target either the insulin or the TCR signaling pathways, and remarkably, nine miRNAs were predicted to target both (miR-103a-3p, miR-193b-5p, miR-197-3p, miR-3187-3p, miR-4302, miR-622, miR-6748-3p, miR-1208, and miR-1292-5p). Among the five miRNAs that alone or in combination predicted 12-month C-peptide outcomes (miR-3187-3p, miR-4302, miR-1292-5p, miR-103a-3p, and miR-4723-5p), four targeted both insulin and TCR signaling pathways and potentially may modulate a large number of genes (71–104 of 139 genes and 65–80 of 110 genes, respectively). For miR-3187-3p, the TCR signaling pathway was predicted as the first of 16 pathways.

DISCUSSION

Despite the emergence of reproducible associations of circulating miRNAs with type 1 diabetes, there are limited data about miRNA prediction of C-peptide decline after diagnosis. Moreover, virtually all published studies of circulating miRNAs in islet autoimmunity and type 1 diabetes used RT-PCR assays investigating a fraction of the known miRNAs (Supplementary Table 1). Nielsen et al. (6) sequenced pooled samples to identify differentially expressed miRNAs between individuals with type 1 diabetes and control subjects and then assessed levels of 24 miRNAs by RT-PCR. With 2,656 transcripts in miRBase V22 (34), there is much potential for discovery. Thus, we profiled 2,083 miRNAs using RNA-seq technology. To date, our study has examined the largest number of miRNAs concerning residual C-peptide at diagnosis.

To investigate whether circulating miRNAs are associated with and predict loss of insulin secretion after diagnosis, we examined fasting serum samples obtained on the same day of the baseline MMTT from 53 individuals. Several miRNAs were associated with C-peptide AUC and/or peak at the baseline MMTT (Table 2 and Fig. 1). miRNA expression quartiles identified subjects with better or worse residual insulin secretion after adjustment for age, sex, and BMI. The observed differences were not explained by variation in time from diagnosis to baseline MMTT (data not shown). These associations survived correction for multiple comparisons by bootstrapping.

In longitudinal analyses, baseline levels of five of these miRNAs, alone or in combination, predicted MMTT C-peptide outcomes at the 12-month visit: miR-3187-3p and miR-4302 predicted C-peptide AUC, miR-3187-3p/miR-103a-3p predicted AUC and peak, and miR-1292-5p predicted peak C-peptide; miR-3187-3p/miR-4723-5p predicted subjects being above or below the peak C-peptide trial eligibility threshold at the 12-month visit. The miR-3187-3p/miR-103a-3p combination improved prediction of C-peptide decline compared with baseline C-peptide AUC alone (Fig. 3*D*). Baseline differences in C-peptide AUC or peak were maintained on follow-up after correction for baseline C-peptide, age, sex, and BMI, and decline occurred with similar slopes (Figs. 2 and 3). We cannot discern whether this reflects differences in physical/functional β-cell mass at baseline, in the severity of the autoimmune process, or both.

A prior study of relatives at risk for type 1 diabetes showed that plotting C-peptide AUC against glucose AUC values at the time points of the oral glucose tolerance test helps with assessing metabolic impairment during progression to clinical diagnosis (40). Changes in the curves' position, shape, and direction demonstrated progressive worsening during the progression. For the first time, we applied this approach to visualize these relationships during the MMTT and analyze differences in metabolic responses at baseline and on follow-up in groups stratified by baseline miRNA levels (Fig. 4).

Subjects having higher baseline C-peptide AUC after miRNA stratification had less pathological curves: Their position on the grid indicated higher C-peptide and lower glucose levels, and their shape indicated more C-peptide secretion relative to glucose levels. On follow-up, their curves remained distinct from those of the other participants. The comparisons of the AUC C-peptide/AUC glucose ratios from baseline ratios quantified that the significant worsening and the differences among the groups stratified by the baseline miRNA levels persisted over time.

For most of the 31 miRNAs associated with C-peptide at baseline, there is no prior involvement in disease-relevant pathways. This is not surprising given that we identified many miRNAs never before examined in this setting. However, miRWalk 2.0 predicted that 19 of 31 miRNAs

are reported in Supplementary Table 2. *D*: Illustration of improved ability to separate between groups with C-peptide decline less or greater than 25% when the miR-3187-3p/miR-103a combination is considered in the model. ROC AUC in the model with and without miRNAs were 0.82 and 0.70, respectively ($P = 0.04$).

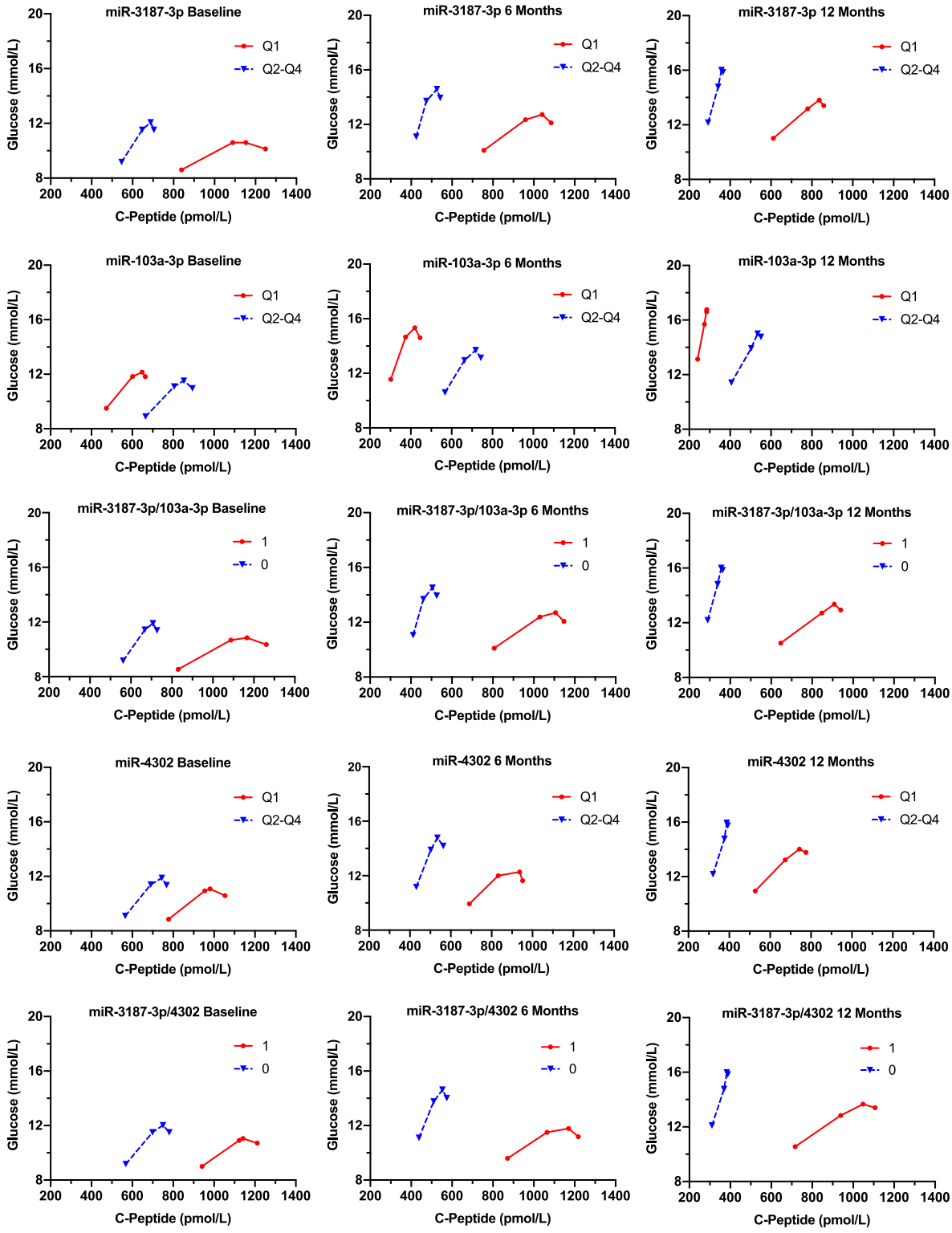

Figure 4— MMTT C-peptide/glucose response (CGR) curves after stratification for baseline miRNA expression quartiles. The curves plot the mean values at 30, 60, 90, and 120 min (left to right) for the baseline, 6-month, and 12-month MMTTs. CGR curves are shown for miR-3187-3p, miR-103a-3p, miR-4302, and the combination of miR-3187-3p with miR-103a-3p (combination 0 = quartile 1 [Q1] miR-103a-3p + Q2–4 miR-3187-3p; combination 1 = Q2–4 miR-103a-3p + Q1 miR-3187-3p) and the combination of miR-3187-3p with miR-4302 (combination 0 = Q2–4 miR-3187-3p + Q2–4 miR-4302; combination 1 = Q1 miR-3187-3p + Q1 miR-4302). Subjects were stratified for baseline expression levels of associated miRNAs; those in the Q1 group had a more monotonic shape of the CGR curves, which is located upward and to the left of subjects in the Q2–Q4 groups. The 6- and 12-month panels show the metabolic deterioration over time in both groups, as is evident by the increasing monotonicity in both and by the upward and leftward movement of the CGR curves.

Table 4—Prediction of targeted gene pathways by miRNAs associated with baseline MMTT AUC and/or peak C-peptide

miRNA	Predicted disease–relevant KEGG pathways	Predicted gene targets/genes in pathway	Pathway ranking	*P* value
miR-98-3p	Insulin signaling	63/139	17 of 18	0.0320
miR-99a-5p	Insulin signaling	34/139	5 of 6	0.0569
miR-103a-3p	Insulin signaling	104/139	2 of 20	8.33E-06
	TCR signaling	80/110	11 of 20	0.0018
miR-127-3p	Insulin signaling	80/139	5 of 21	0.0002
miR-193b-5p	TCR signaling	94/110	13 of 27	0.0005
	Insulin signaling	115/139	16 of 27	0.0013
miR-197-3p	TCR signaling	59/110	8 of 18	0.0046
	Insulin signaling	71/139	10 of 18	0.0064
miR-2355-3p	Insulin signaling	84/139	14 of 14	0.0469
miR-342-3p	Insulin signaling	90/139	1 of 23	5.00E-06
miR-622	TCR signaling	82/110	15 of 33	0.0002
	Insulin signaling	100/139	16 of 33	0.0003
	Type 2 diabetes	38/49	31 of 33	0.0381
miR-934	Insulin signaling	76/139	5 of 17	0.0017
miR-1208	Insulin signaling	91/139	4 of 27	5.14E-05
	TCR signaling	72/110	14 of 27	0.0008
	Type 2 diabetes	36/49	17 of 27	0.0049
miR-1292-5p	Insulin signaling	91/139	10 of 22	0.0008
	TCR signaling	71/110	17 of 22	0.0171
miR-3187-3p	Insulin signaling	101/139	1 of 16	4.76E-06
	TCR signaling	74/110	12 of 16	0.0230
miR-4302	Insulin signaling	85/139	6 of 19	0.0001
	TCR signaling	65/110	12 of 19	0.0094
miR-4304	Insulin signaling	57/139	3 of 15	0.0001
miR-4723-5p	Insulin signaling	71/139	2 of 20	3.40E-06
	Type 2 diabetes	28/49	16 of 20	4.72E-03
miR-6748-3p	TCR signaling	49/110	9 of 21	0.0005
	Insulin signaling	57/139	12 of 21	0.0021
miR-7154-3p	Insulin signaling	76/139	3 of 12	0.0008
	SNARE interactions in vesicular transport	26/29	8 of 12	0.0160
miR-8058	Insulin signaling	60/139	5 of 12	0.0002

Disease-relevant gene pathways predicted to be targeted by miRNAs associated with C-peptide in the primary analysis. Number of predicted genes, ranking of the reported pathways, and corrected *P* values are shown. KEGG, Kyoto Encyclopedia of Genes and Genomes.

may target disease-relevant gene pathways; 7 of 19 had previous disease-relevant literature associations (4 with type 1 and type 2 diabetes, 2 with type 2 diabetes only, and 1 with β-cell differentiation). Remarkably, 19 miRNAs could target either the insulin or the TCR signaling pathway; 9 miRNAs may target both. These included four of five miRNAs associated with C-peptide at the 12-month MMTT alone or in combination (miR-3187-3p, miR-4302, miR-103a-3p, miR-1292-5p, and miR-4723-5p). There were no previous associations, except for miR-589-5p, for 13 miRNAs with no relevant predictions.

miR-3187-3p had the strongest association with C-peptide. The TCR signaling pathway ranked first of 16 predicted pathways. It could target genes involved in AKT (serine/threonine kinase)/phosphatidylinositol 3-kinase signaling, which is critical for the development, differentiation, and function of effector (41) and regulatory (42) T cells. Other predicted targets include the CD3 γ-chain, the *MAPK13* and *MAPK14* genes in the mitogen-activated protein kinase signaling pathway, *LAT* (linker for the activation of T cells), *SOS1* (son of sevenless factor 1, an exchange factor recruited by *LAT*), *NFAT* (transcription factor nuclear factor of activated T cells), and *PTPRC* (the tyrosine phosphatase CD45) (43).

Plasma levels of miR-103a-3p were increased in individuals with type 1 diabetes (<5 years duration compared with healthy subjects) (18). We show that higher miR-103a-3p levels are associated with higher residual insulin

secretion near diagnosis and that baseline miR-103a-3p levels can aid in predicting C-peptide AUC at 12 months; the combination miR-3187-3p/miR-103a-3p was the stronger predictor of C-peptide AUC. This miRNA was linked to type 2 diabetes, obesity, and HFN1A maturity-onset diabetes of the young (44–46). In the Coronary Diet Intervention with Olive Oil and Cardiovascular Prevention study, low circulating levels of miR-103a-3p were associated with increased likelihood of type 2 diabetes (47). miR-107 and miR-103a-3p are negative regulators of insulin sensitivity (48). Validated gene targets of miR-103a-3p include *SFRP4* (the secreted frizzled-related protein 4), which suppresses insulin exocytosis (49), and *CAV1* (caveolin 1), which inhibits insulin signaling by decreasing insulin receptors in caveolae-enriched plasma membrane domains (48). miR-103a-3p regulates the autophagy gene *ATG5* (50), and autophagy regulates transport-competent secretory peptide precursors, including proinsulin (51). In our analysis, this miRNA may target both the TCR and the insulin signaling pathways.

Other miRNAs were associated with C-peptide at baseline but not on follow-up. These included miR-197-3p, which in a previous report predicted future C-peptide AUC (12); the different outcomes may reflect assay type, sample size (most likely), or sample type (serum vs. plasma). miR-197-3p is predicted to target several genes in both the insulin and the TCR signaling pathways. Its plasma levels were reduced in subjects with type 2 diabetes (52).

The gene coding for miR-342-3p on 14q32 contains a cluster of glucose-responsive miRNAs expressed in pancreatic islet cells (53); miR-342-3p also regulates the expression of the autoantigen IA-2β (54). We previously reported that miR-342-3p levels were associated with an increased risk of progression to type 1 diabetes among autoantibody-positive relatives, and levels correlated with oral glucose tolerance test outcomes (13); in other studies, miR-342-3p was differentially expressed in individuals with type 1 diabetes compared with healthy subjects and at-risk relatives (14); its levels were reduced in regulatory T cells in affected individuals compared with healthy subjects (25).

miR-127-3p is enriched in human β-cells (55) and involved in endocrine differentiation (56); miR-99a-5p exhibited increased levels during the first 12 months postdiagnosis in children with recent-onset type 1 diabetes (20) and targets the mammalian target of rapamycin pathway (57). miR-589-5p (58) and miR-193b-5p were associated with type 2 diabetes and prediabetes, respectively; miR-193b-5p was linked to islet autoimmunity because it was differentially expressed in autoantibody-positive versus -negative individuals (10).

In closing, trial subjects with higher or lower MMTT C-peptide AUC and peak were stratified by baseline miRNA levels. Selected miRNAs/miRNA combinations predicted future decline of C-peptide AUC and peak. Predicting future C-peptide at baseline is critical for subject stratification early after diagnosis when impactful decisions about trial participation or treatment need to be made. An miRNA combination predicted 12-month C-peptide peak above/below the clinical trial eligibility threshold, which is of particular importance given increased consideration for trial enrollment up to 2 years from diagnosis if meeting the peak C-peptide threshold. Many associated miRNAs were examined for the first time, but some were previously linked to type 1 diabetes; several are predicted to affect gene pathways relevant to β-cell function and T cells, both critical to disease pathogenesis. Future studies may explore possible links of miRNAs with disease endotypes. Limitations of this study are the limited sample size and the lack of a validation cohort, which require future investigations. These miRNAs are excellent candidates for validation studies and may become useful biomarkers for advancing therapeutic discoveries for type 1 diabetes.

Acknowledgments. We acknowledge Simi Ahmed (JDRF) for programmatic support.

Funding. The study was supported by JDRF (2-SRA-2015-122-Q-R) and the Diabetes Research Institute Foundation, Hollywood, Florida. We acknowledge the support of the Type 1 Diabetes TrialNet Study Group, which identified study subjects and provided samples and follow-up data for this study. The Type 1 Diabetes TrialNet Study Group is a clinical trials network funded by the National Institutes of Health through the National Institute of Diabetes and Digestive and Kidney Diseases, the National Institute of Allergy and Infectious Diseases, and the *Eunice Kennedy Shriver* National Institute of Child Health and Human Development through cooperative agreements U01-DK-061010, U01-DK-061034, U01-DK-061042, U01-DK-061058, U01-DK-085453, U01-DK-085461, U01-DK-085465, U01-DK-085466, U01-DK-085476, U01-DK-085499, U01-DK-085504, U01-DK-085509, U01-DK-103180, U01-DK-103153, U01-DK-103266, U01-DK-103282, U01-DK-106984, U01-DK-106994, U01-DK-107013, U01-DK-107014, UC4-DK-106993, UC4-DK-11700901, and U01-DK-106693-02 and through JDRF.

The contents of this article are solely the responsibility of the authors and do not necessarily represent the official views of the National Institutes of Health or JDRF.

Duality of Interest. No potential conflicts of interest relevant to this article were reported.

Author Contributions. I.S. generated the data. I.S., R.P., J.S., S.M.C., and A.P. analyzed and interpreted data and participated in the preparation of the manuscript and approved its final version. R.P., J.S., S.M.C., and A.P conceived the study or parts of the study. S.M.C. was responsible for statistical design and the analysis plan. S.M.C. and A.P. are the guarantors of this work and, as such, had full access to all the data in the study and take responsibility for the integrity of the data and the accuracy of the data analysis.

References

1. Rodriguez-Calvo T, Richardson SJ, Pugliese A. Pancreas pathology during the natural history of type 1 diabetes. Curr Diab Rep 2018;18:124

2. Greenbaum CJ, Beam CA, Boulware D, et al.; Type 1 Diabetes TrialNet Study Group. Fall in C-peptide during first 2 years from diagnosis: evidence of at least two distinct phases from composite Type 1 Diabetes TrialNet data. Diabetes 2012; 61:2066–2073

3. Warshauer JT, Bluestone JA, Anderson MS. New frontiers in the treatment of type 1 diabetes. Cell Metab 2020;31:46–61

4. Yates LA, Norbury CJ, Gilbert RJ. The long and short of microRNA. Cell 2013; 153:516–519

5. Kroh EM, Parkin RK, Mitchell PS, Tewari M. Analysis of circulating microRNA biomarkers in plasma and serum using quantitative reverse transcription-PCR (qRT-PCR). Methods 2010;50:298–301

6. Nielsen LB, Wang C, Sørensen K, et al. Circulating levels of microRNA from children with newly diagnosed type 1 diabetes and healthy controls: evidence that miR-25 associates to residual beta-cell function and glycaemic control during disease progression. Exp Diabetes Res 2012;2012:896362
7. Latreille M, Herrmanns K, Renwick N, et al. miR-375 gene dosage in pancreatic β-cells: implications for regulation of β-cell mass and biomarker development. J Mol Med (Berl) 2015;93:1159–1169
8. Marchand L, Jalabert A, Meugnier E, et al. miRNA-375 a sensor of glucotoxicity is altered in the serum of children with newly diagnosed type 1 diabetes. J Diabetes Res 2016;2016:1869082
9. Seyhan AA, Nunez Lopez YO, Xie H, et al. Pancreas-enriched miRNAs are altered in the circulation of subjects with diabetes: a pilot cross-sectional study. Sci Rep 2016;6:31479
10. Yin CW, Weiland M, Li J, She R, Zhiu L, Mi Q. Serum miRNAs as potential biomarkers for early prediction of type 1 diabetes. FASEB J 2016;30(Suppl. 1):307.3
11. Erener S, Marwaha A, Tan R, Panagiotopoulos C, Kieffer TJ. Profiling of circulating microRNAs in children with recent onset of type 1 diabetes. JCI Insight 2017;2:e89656
12. Samandari N, Mirza AH, Nielsen LB, et al. Circulating microRNA levels predict residual beta cell function and glycaemic control in children with type 1 diabetes mellitus. Diabetologia 2017;60:354–363
13. Snowhite IV, Allende G, Sosenko J, Pastori RL, Messinger Cayetano S, Pugliese A. Association of serum microRNAs with islet autoimmunity, disease progression and metabolic impairment in relatives at risk of type 1 diabetes. Diabetologia 2017;60:1409–1422
14. Åkerman L, Casas R, Ludvigsson J, Tavira B, Skoglund C. Serum miRNA levels are related to glucose homeostasis and islet autoantibodies in children with high risk for type 1 diabetes. PLoS One 2018;13:e0191067
15. Lakhter AJ, Pratt RE, Moore RE, et al. Beta cell extracellular vesicle miR-21-5p cargo is increased in response to inflammatory cytokines and serves as a biomarker of type 1 diabetes. Diabetologia 2018;61:1124–1134
16. Grieco GE, Cataldo D, Ceccarelli E, et al. Serum levels of miR-148a and miR-21-5p are increased in type 1 diabetic patients and correlated with markers of bone strength and metabolism. Noncoding RNA 2018;4:37
17. Liu L, Yan J, Xu H, et al. Two novel MicroRNA biomarkers related to β-cell damage and their potential values for early diagnosis of type 1 diabetes. J Clin Endocrinol Metab 2018;103:1320–1329
18. Assmann TS, Recamonde-Mendoza M, Puñales M, Tschiedel B, Canani LH, Crispim D. MicroRNA expression profile in plasma from type 1 diabetic patients: case-control study and bioinformatic analysis. Diabetes Res Clin Pract 2018;141:35–46
19. Małachowska B, Wyka K, Nowicka Z, Bartłomiejczyk MA, Młynarski W, Fendler W. Temporal dynamics of serum let-7g expression mirror the decline of residual beta-cell function in longitudinal observation of children with type 1 diabetes. Pediatr Diabetes 2018;19:1407–1415
20. Samandari N, Mirza AH, Kaur S, et al. Influence of disease duration on circulating levels of miRNAs in children and adolescents with new onset type 1 diabetes. Noncoding RNA 2018;4:35
21. Bertoccini L, Sentinelli F, Incani M, et al. Circulating miRNA-375 levels are increased in autoantibodies-positive first-degree relatives of type 1 diabetes patients. Acta Diabetol 2019;56:707–710
22. Liu Y, Ma M, Yu J, et al. Decreased serum *microRNA-21*, *microRNA-25*, *microRNA-146a*, and *microRNA-181a* in autoimmune diabetes: potential biomarkers for diagnosis and possible involvement in pathogenesis. Int J Endocrinol 2019;2019:8406438
23. Garavelli S, Bruzzaniti S, Tagliabue E, et al. Blood co-circulating extracellular microRNAs and immune cell subsets associate with type 1 diabetes severity. Int J Mol Sci 2020;21:477
24. Garavelli S, Bruzzaniti S, Tagliabue E, et al. Plasma circulating miR-23∼27∼24 clusters correlate with the immunometabolic derangement and predict C-peptide loss in children with type 1 diabetes. Diabetologia 2020;63:2699–2712
25. Hezova R, Slaby O, Faltejskova P, et al. microRNA-342, microRNA-191 and microRNA-510 are differentially expressed in T regulatory cells of type 1 diabetic patients. Cell Immunol 2010;260:70–74
26. Roggli E, Gattesco S, Caille D, et al. Changes in microRNA expression contribute to pancreatic β-cell dysfunction in prediabetic NOD mice. Diabetes 2012;61:1742–1751
27. Serr I, Fürst RW, Ott VB, et al. miRNA92a targets KLF2 and the phosphatase PTEN signaling to promote human T follicular helper precursors in T1D islet autoimmunity. Proc Natl Acad Sci U S A 2016;113:E6659–E6668
28. Serr I, Scherm MG, Zahm AM, et al. A miRNA181a/NFAT5 axis links impaired T cell tolerance induction with autoimmune type 1 diabetes. Sci Transl Med 2018;10:eaag1782
29. Scherm MG, Serr I, Zahm AM, et al. miRNA142-3p targets Tet2 and impairs Treg differentiation and stability in models of type 1 diabetes. Nat Commun 2019;10:5697
30. Guay C, Kruit JK, Rome S, et al. Lymphocyte-derived exosomal microRNAs promote pancreatic β cell death and may contribute to type 1 diabetes development. Cell Metab 2019;29:348–361.e6
31. Xu G, Thielen LA, Chen J, et al. Serum miR-204 is an early biomarker of type 1 diabetes-associated pancreatic beta-cell loss. Am J Physiol Endocrinol Metab 2019;317:E723–E730
32. Greenbaum CJ, Mandrup-Poulsen T, McGee PF, et al.; Type 1 Diabetes Trial Net Research Group; European C-Peptide Trial Study Group. Mixed-meal tolerance test versus glucagon stimulation test for the assessment of beta-cell function in therapeutic trials in type 1 diabetes. Diabetes Care 2008;31:1966–1971
33. Godoy PM, Barczak AJ, DeHoff P, et al. Comparison of reproducibility, accuracy, sensitivity, and specificity of miRNA quantification platforms. Cell Rep 2019;29:4212–4222.e5
34. Kozomara A, Birgaoanu M, Griffiths-Jones S. miRBase: from microRNA sequences to function. Nucleic Acids Res 2019;47:D155–D162
35. Law CW, Chen Y, Shi W, Smyth GK. voom: precision weights unlock linear model analysis tools for RNA-seq read counts. Genome Biol 2014;15:R29
36. Ritchie ME, Phipson B, Wu D, et al. limma powers differential expression analyses for RNA-sequencing and microarray studies. Nucleic Acids Res 2015;43:e47
37. Anders S, Pyl PT, Huber W. HTSeq–a Python framework to work with high-throughput sequencing data. Bioinformatics 2015;31:166–169
38. DeLong ER, DeLong DM, Clarke-Pearson DL. Comparing the areas under two or more correlated receiver operating characteristic curves: a nonparametric approach. Biometrics 1988;44:837–845
39. Dweep H, Gretz N. miRWalk2.0: a comprehensive atlas of microRNA-target interactions. Nat Methods 2015;12:697
40. Sosenko JM, Skyler JS, Herold KC, et al.; Type 1 Diabetes TrialNet Study Group. Slowed metabolic decline after 1 year of oral insulin treatment among individuals at high risk for type 1 diabetes in the Diabetes Prevention Trial-Type 1 (DPT-1) and TrialNet oral insulin prevention trials. Diabetes 2020;69:1827–1832
41. Han JM, Patterson SJ, Levings MK. The role of the PI3K signaling pathway in CD4(+) T cell differentiation and function. Front Immunol 2012;3:245
42. Sauer S, Bruno L, Hertweck A, et al. T cell receptor signaling controls Foxp3 expression via PI3K, Akt, and mTOR. Proc Natl Acad Sci U S A 2008;105:7797–7802
43. Vignard V, Labbé M, Marec N, et al. MicroRNAs in tumor exosomes drive immune escape in melanoma. Cancer Immunol Res 2020;8:255–267
44. Luo M, Xu C, Luo Y, Wang G, Wu J, Wan Q. Circulating miR-103 family as potential biomarkers for type 2 diabetes through targeting CAV-1 and SFRP4. Acta Diabetol 2020;57:309–322
45. Zhu H, Leung SW. Identification of microRNA biomarkers in type 2 diabetes: a meta-analysis of controlled profiling studies. Diabetologia 2015;58:900–911
46. Bonner C, Nyhan KC, Bacon S, et al. Identification of circulating microRNAs in HNF1A-MODY carriers. Diabetologia 2013;56:1743–1751
47. Jiménez-Lucena R, Rangel-Zúñiga OA, Alcalá-Díaz JF, et al. Circulating miRNAs as predictive biomarkers of type 2 diabetes mellitus development in coronary heart disease patients from the CORDIOPREV study. Mol Ther Nucleic Acids 2018;12:146–157

48. Trajkovski M, Hausser J, Soutschek J, et al. MicroRNAs 103 and 107 regulate insulin sensitivity. Nature 2011;474:649–653
49. Mahdi T, Hänzelmann S, Salehi A, et al. Secreted frizzled-related protein 4 reduces insulin secretion and is overexpressed in type 2 diabetes. Cell Metab 2012;16:625–633
50. Zhang C, Zhang C, Wang H, Qi Y, Kan Y, Ge Z. Effects of miR-103a-3p on the autophagy and apoptosis of cardiomyocytes by regulating Atg5. Int J Mol Med 2019;43:1951–1960
51. Riahi Y, Wikstrom JD, Bachar-Wikstrom E, et al. Autophagy is a major regulator of beta cell insulin homeostasis. Diabetologia 2016;59:1480–1491
52. Zampetaki A, Kiechl S, Drozdov I, et al. Plasma microRNA profiling reveals loss of endothelial miR-126 and other microRNAs in type 2 diabetes. Circ Res 2010;107:810–817
53. Kameswaran V, Bramswig NC, McKenna LB, et al. Epigenetic regulation of the DLK1-MEG3 microRNA cluster in human type 2 diabetic islets. Cell Metab 2014;19:135–145
54. Abuhatzira L, Xu H, Tahhan G, Boulougoura A, Schäffer AA, Notkins AL. Multiple microRNAs within the 14q32 cluster target the mRNAs of major type 1 diabetes autoantigens IA-2, IA-2β, and GAD65. FASEB J 2015;29:4374–4383
55. Klein D, Misawa R, Bravo-Egana V, et al. MicroRNA expression in alpha and beta cells of human pancreatic islets. PLoS One 2013;8:e55064
56. Jin W, Mulas F, Gaertner B, et al. A network of microRNAs acts to promote cell cycle exit and differentiation of human pancreatic endocrine cells. iScience 2019;21:681–694
57. Tsai TF, Lin JF, Chou KY, Lin YC, Chen HE, Hwang TI. miR-99a-5p acts as tumor suppressor via targeting to mTOR and enhances RAD001-induced apoptosis in human urinary bladder urothelial carcinoma cells. OncoTargets Ther 2018;11:239–252
58. Mononen N, Lyytikäinen LP, Seppälä I, et al. Whole blood microRNA levels associate with glycemic status and correlate with target mRNAs in pathways important to type 2 diabetes. Sci Rep 2019;9:8887